

UDC 004.94(045)
DOI:10.18372/1990-5548.88.20963

¹Oleksii Kosiuk,
²Olena Chumachenko

SYNTHETIC CT GENERATION FOR CARDIOTHORACIC INJURIES WITH INTRACARDIAC FOREIGN BODIES

National Technical University of Ukraine "Ihor Sikorsky Kyiv Polytechnic Institute," Kyiv, Ukraine
E-mails: ¹kosiuk.o.m.-ki51f@edu.kpi.ua ORCID 0009-0001-6647-9558,
²eliranvik@gmail.com ORCID 0000-0003-3006-7460

Abstract—This paper proposes novel methods for the generation of synthetic CT images of cardiothoracic injuries with foreign bodies (FB) localized in the cardiac region. These methods are intended to improve the FB segmentation performance by machine learning models through the augmentation of training datasets with synthetic images. A small real-world dataset was collected, consisting of 8 CT scans of combat cardiothoracic injuries with foreign bodies (FB amount ranging from 1 to 3) localized in the heart area, and an additional 4 "clean" CT scans of blast-induced cardiothoracic injuries where foreign bodies are absent in the cardiac region. Through the analysis of the collected dataset and findings from similar studies, the morphology of foreign bodies and the statistics of their localization in the heart during combat cardiothoracic trauma were examined. Two methods for synthesizing artificial CT images of cardiothoracic injuries with heart-localized FBs based on clean CT scans were developed: *RealInsFB-CT*, based on the insertion of regions of interest extracted from real injury CT scans-containing FB, artifacts, and surrounding damaged tissues – into clean CT scans and *MorphGenFB-CT*, based on the morphologically and statistically grounded generation of a 3D FB model, filling the model with Hounsfield Unit values corresponding to the selected FB material, inserting the model into one of the heart chambers on a clean CT scan, and the artificial generation of artifacts. Using both methods, CT images were synthesized and compiled into training datasets (19 CT scans + 19 FB masks each). The visual, structural, and statistical similarity between real and synthesized CT scans was proved.

Keywords—Synthetic data, data augmentation, segmentation, foreign bodies, cardiothoracic injury, computed tomography.

I. INTRODUCTION

The full-scale Russian invasion of Ukraine has presented military medicine with unprecedented challenges. Specifically, there is a growing need for treating penetrating gunshot and blast-induced chest injuries that significantly damage the cardiovascular system. Such injuries are often accompanied by the localization of foreign bodies (FBs), such as shrapnel and bullets, within or adjacent to the heart and major blood vessels.

Among all combat traumas, chest injuries account for 10–12%, while injuries to the heart and great vessels comprise 3–4%. Although this percentage is relatively small, it carries the highest mortality rate—exceeding 80% at the pre-hospital stage. Foreign bodies are identified in 15–20% of all penetrating heart injuries. Furthermore, the presence of an FB increases mortality risks (approaching 90%) due to the severe complications of late-onset sepsis, myocardial abscess, and cardiac tamponade.

Treatment efficacy is determined by timely diagnosis and evidence – based surgical tactics, with Computed Tomography (CT) serving as the "gold standard." However, the lack of complex, low-

mobility diagnostic equipment in field conditions, combined with a shortage of highly qualified medical specialists near the front line, limited time, and high stress levels, often leads to suboptimal surgical decisions. The application of Machine Learning (ML) and Deep Learning (DL) offers new possibilities for diagnosing penetrating chest wounds and detecting FBs in the cardiac region. This allows for: first, offloading medical personnel by delegating diagnostic and surgical planning tasks to an AI-based automated system; and second, providing clinicians with a means to verify their own medical conclusions, thereby minimizing errors and reducing psychological pressure.

One of the initial diagnostic stages in planning FB removal surgeries is FB segmentation. This process helps determine critical spatial features, such as the FB's linear dimensions, volume, and spatial configuration relative to heart chambers and major vessels. The primary challenge in segmenting intracardiac foreign bodies using ML methods is not a lack of specialized architectures – as many approaches ranging from 3D U-Net to ViT and GNN have been developed – but rather the scarcity of real CT scans data. This scarcity is driven by the

relatively low percentage of heart injuries, the high pre-hospital mortality rate, and regulatory restrictions limiting researcher access to sensitive medical and military data. Consequently, the only viable solution to this problem is the synthetic CT images generation of images mimicking original patient scans to augment real-world training datasets.

II. REVIEW OF PUBLICATIONS

Current research on the nature of military conflicts and combat trauma statistics in Ukraine (2014–2026) and worldwide demonstrates a gradual shift in the structure of battlefield injuries. Unlike conflicts of the previous century, blast-induced trauma has become the dominant wounding factor, accounting for approximately 70–85% of all injuries. The proportion of gunshot wounds ranges from 10% to 22% [4] [9] [16].

Analysis of combat trauma statistics indicates that chest injuries comprise 10–12% of all battlefield wounds, ranking third in frequency after injuries to the extremities and the head. Approximately half of these (5–6%) are severe penetrating injuries, and a quarter (3–4%) are accompanied by damage to the heart and great vessels (cardiothoracic trauma) [2] [10]. Among blast-induced and shrapnel chest wounds, 58–60% are blind (retained) injuries, compared to approximately 12% for gunshot wounds [16].

Regarding the distribution of foreign body (FB) localization in blind penetrating chest wounds, approximately one-quarter of FBs affect the heart or major blood vessels. Most frequently, foreign bodies are located within the myocardium or the cavities of the right (45%) and left (35%) ventricles, while atrial involvement (primarily the right atrium) is significantly less common. Among the great vessels, FBs are most often found within or adjacent to the pulmonary artery and less frequently near the vena cava and the aorta; nearly all cases of aortic damage in combat conditions are fatal, with the wounded often dying at the pre-hospital stage before medical imaging, specifically CT, can be performed [1] [2] [3] [7] [16].

Based on contemporary studies of FB morphology in blind combat cardiothoracic injuries, it can be established that FBs primarily exhibit cylindrical (52%), spherical (21%), flat-plate (15%), or irregular jagged (12%) shapes. The linear dimensions of foreign bodies vary from 0.5 mm to several dozen millimeters, and their weight ranges from 8 mg to 37.6 g. A typical FB (80% of cases) has linear dimensions between 2 mm and 12 mm and a weight between 0.3 g and 1 g. Almost all (93%) FBs are metallic, while the remainder – including

secondary fragments – consist of plastic, wood, glass, and other non-metallic materials [7] [15].

The foundation of modern emergency diagnostics for cardiothoracic injuries is the eFAST protocol [8], which enables the detection of free fluid (blood) within body cavities via ultrasound within 2–5 minutes. This allows for rapid conclusions regarding internal bleeding and informs critical decisions on the necessity of urgent surgery. However, due to the acoustic shadow phenomenon, it is impossible to clearly segment a foreign body using ultrasound in cases of blind (retained) heart injuries.

For the detection and precise segmentation of foreign bodies, Computed Tomography (CT) remains the only effective medical imaging modality. The primary challenges in FB segmentation within CT scans are the presence of streaking (radiational) and motion artifacts. Such artifacts distort the image and limit the efficacy of simple segmentation methods, such as Hounsfield Unit (HU) thresholding, necessitating the use of more complex and universal approaches. It is also crucial to consider that most modern CT scan results are clipped at a maximum value of $HU = +3071$ (the saturation effect). This limits the represented radiodensity of steel (typically $HU = 10,000–18,000$) to values close to those of certain metallic artifacts or dense cortical bone ($HU = 1,900–3,500$), further restricting the utility of threshold-based methods and simple filters.

Several distinct methods are utilized for the segmentation of foreign bodies (FBs) within the chest, and specifically within the heart. The most basic among them are threshold segmentation and adaptive filtering; while these are computationally simple and fast, they prove ineffective in the presence of artifacts or in cases where the radiodensity of the foreign body is equal to that of the surrounding tissues.

Machine learning methods offer greater versatility and artifact tolerance. Utilizing ML models based on architectures ranging from 3D U-Net to Vision Transformers (ViT) can yield relatively accurate results, provided there is a sufficient quantity and quality of training data. Recently, the nnU-Net framework [17] was developed, which performs automated data preprocessing, augmentation, and hyperparameter tuning prior to training a U-Net-based model. Furthermore, the use of lightweight CNN architectures shows promise for solving specific tasks such as FB segmentation, detection, or classification from various imaging modalities, including ultrasound [18].

While the scarcity of medical data, particularly CT scans, for training ML models is a widespread issue, research specifically focused on data synthesis and augmentation to improve the accuracy of foreign body (FB) segmentation in the chest and heart is nearly non-existent. A study was recently published exploring the generation of synthetic X-ray images and their use in augmenting real-world data to enhance FB detection accuracy in the thoracic region [19]. The study demonstrates that a model trained on a real-world dataset augmented with synthetic images achieves higher detection accuracy than a model trained solely on real images. Furthermore, the X-ray synthesis method – based on inserting FB images into clean scans followed by the physical modeling of artifacts – yields significantly better results than approaches based on diffusion models.

III. PROBLEM STATEMENT

The objective of this work is to investigate the epidemiology, statistics, and morphology of penetrating cardiothoracic injuries characterized by the localization of foreign bodies within the heart and/or near major blood vessels, and to develop methods for synthesizing artificial CT scans images. These synthetic images are intended to augment limited real-world datasets to improve the accuracy of foreign body segmentation in the heart using state-of-the-art machine learning methods and models.

To achieve the objective of this work, the following tasks must be addressed.

Development of image synthesis methods for injury CT scans with Foreign Bodies (FBs): create algorithms for generating 3D models of foreign bodies that incorporate the morphological statistics of combat injuries (shapes, sizes, and materials of fragments, with a focus on metallic materials) and methods for inserting synthetic objects into real CT scans ("clean" donor images), which includes:

- imitating the saturation effect at the + 3071 HU level to reproduce the real behavior of the scanner detector;
- algorithmic modeling of metal artifacts (streaking artifacts) that arise around metallic fragments and distort the surrounding myocardial tissues;
- inserting the synthetic fragment into one of the four cardiac chambers (left ventricle, right ventricle, left atrium, right atrium) with probabilities corresponding to the distributions found in real-world clinical studies.

More formally: for a dataset of real CT scans of cardiothoracic injuries with FBs localized in the

cardiac region, $CT_{inj} = \left\{ \left(X_i^{(inj)}, Y_i^{(inj)} \right) \right\}_{i=1}^{N_{inj}}$, where each CT scan $X_i^{(inj)} \in \{n \in \mathbb{Z} | -1000 \leq n \leq 3071\}^{H_i \times W_i \times D_i}$ is a 3D tensor with dimensions $H_i \times W_i \times D_i$, and each binary mask of the region of injury (ROI) including the FB and wounded tissues $Y_i^{(inj)} \in \{0,1\}^{h_i \times w_i \times d_i}$ is a 3D tensor with dimensions $h_i \times w_i \times d_i$; and for a sample of "clean" real cardiothoracic CT scans without foreign bodies $CT_{clean} = \left\{ X_i^{(clean)} \right\}_{i=1}^{N_{clean}}$ where each scan $X_i^{(clean)} \in \{n \in \mathbb{Z} | -1000 \leq n \leq 3071\}^{H_i \times W_i \times D_i}$ is a 3D tensor with dimensions $H_i \times W_i \times D_i$:

1) For each "clean" CT scan from CT_{clean} obtain a cardiac mask forming a sample of cardiac masks $M_{heart} = \left\{ M_i^{(heart)} \right\}_{i=1}^{N_{clean}}$, where each cardiac mask $M_i^{(heart)} \in \{0,4\}^{h_i \times w_i \times d_i}$ is a 3D tensor where 0 represents the background, 1 is the left ventricle, 2 is the left atrium, 3 is the right ventricle, and 4 is the right atrium. This can also be represented as a set of 3D tensors for each cardiac chamber $M_{heart} = \left\{ M_i^{(lv)}, M_i^{(la)}, M_i^{(rv)}, M_i^{(ra)} \right\}_{i=1}^{N_{clean}}$.

2) Generate a sample of foreign bodies (injury ROIs with FBs) $S_{FB} = \left\{ X_i^{(FB)} \right\}_{i=1}^{N_{FB}}$, where $X_i^{(FB)} \in \{0,1\}^{h_i \times w_i \times d_i}$ is a 3D model of the foreign body or ROI.

3) Based on the samples CT_{clean} , M_{heart} , and S_{FB} synthesize a labeled dataset of injury CT scans with generated FBs (ROIs) $CT_{synth} = \left\{ \left(X_i^{(synth)}, M_i^{(heart)}, Y_i^{(synth)} \right) \right\}_{i=1}^{N_{synth}}$ via inserting the generated FB (ROI) from S_{FB} sample into a clean CT scan from CT_{clean} sample for the creation of each synthetic CT scan $X_i^{(synth)} \in \{n \in \mathbb{Z} | -1000 \leq n \leq 3071\}^{H_i \times W_i \times D_i}$ such that the FB mask $Y_i^{(synth)} \in \{0,1\}^{h_i \times w_i \times d_i}$ is entirely contained within the corresponding mask of the cardiac chamber selected for insertion

$$\begin{aligned} M_i^{(ch)} &\in M_{heart} : \\ \exists! M_i^{(ch)} &\in \{M_i^{(lv)}, M_i^{(la)}, M_i^{(rv)}, M_i^{(ra)}\} : \\ Y_i^{(synth)} &\subseteq M_i^{(ch)}. \end{aligned}$$

Evaluation of Synthetic CT Image Realism: To demonstrate the morphological and statistical fidelity of synthetic CT scans compared to the gold

standard (real-world images) through HU histogram analysis.

IV. PROPOSED METHODS AND RESULTS

The first method, RealInsFB-CT, consists of extracting volumetric regions of injury (ROIs) containing the foreign body, its associated artifacts, and the surrounding tissues from real-world injury CT scans $X_i^{(inj)}$ of CT_{inj} based on $Y_i^{(inj)}$ masks. These fragments are then inserted—with random rotation and Gaussian blurring of the tissue boundaries—into a randomly selected cardiac chamber on a "clean" real-world CT scan $X_i^{(clean)}$ based on the statistical distribution of FB localization in clinical injuries (e.g., the probability of fragment insertion into the right ventricle is 45%). The ROI can be entirely inserted ($Y_i^{(synth)} \subseteq M_i^{(ch)}$) into one of the four cardiac chambers (left ventricle, right ventricle, left atrium, right atrium) according to the following probabilities (Table I).

TABLE I. CARDIAC CHAMBERS FOR ROI INSERTION PROBABILITIES

| Heart Chamber | Insertion Probability |
|-----------------|-----------------------|
| Left Ventricle | 35% |
| Right Ventricle | 5% |
| Left Atrium | 45% |
| Right Atrium | 15% |

The TotalSegmentator model [20] is utilized for the segmentation of cardiac chambers from CT scans and the extraction of their respective masks to facilitate the subsequent insertion of foreign bodies into the heart. An example of a cardiac mask with segmented chambers shown in three projections is illustrated in Fig. 1.

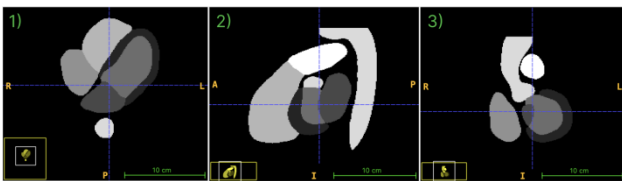


Fig. 1. Cardiac mask with segmented chambers obtained using the TotalSegmentator model: (1) is the axial; (2) is the sagittal; (3) is the coronal

The schematic diagram describing the RealInsFB-CT method is shown in Fig. 2.

The second method, MorphGenFB-CT, involves the generation of 3D foreign body (FB) models ($S_{FB} = \{X_i^{(FB)}\}_{i=1}^{N_{FB}}$) based on statistical data regarding the size and morphology of FBs in

cardiothoracic injuries, followed by their entire insertion ($Y_i^{(synth)} \subseteq M_i^{(ch)}$) into a cardiac chamber from

$$M_{heart} = \{M_i^{(lv)}, M_i^{(ra)}, M_i^{(rv)}, M_i^{(la)}\}_{i=1}^{N_{clean}}$$

randomly selected based on previously mentioned probabilities with random rotation and synthetic artifact generation. This method allows for flexible material selection by filling the 3D model with specific Hounsfield Unit (HU) values corresponding to different materials. For example, for aluminum, HU values ranging from +2000 to +3500 are used and subsequently clipped at +3071 HU, which is the upper limit for most modern CT scanners. When augmenting a specific dataset with synthetic images, it is recommended to use HU values that match the FB materials present in the real-world data. The algorithm implementing the MorphGenFB-CT method consists of the following primary steps.

1) *Generation of 3D Foreign Body Models in Voxel Space*: the method is based on stochastic modeling within a voxel grid with a resolution of 0.5 mm. Base Primitive: An initial geometric primitive (ellipsoid or spindle) is created, with parameters varying based on the specified type: cylindrical, spherical, compact, needle-like (utilizing bending transformations), or plate-like (incorporating random through-hole defects).

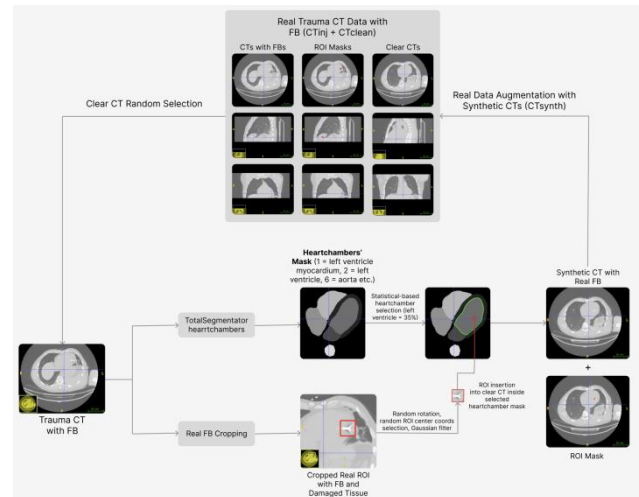


Fig. 2. RealInsFB-CT method

- *Surface Realism*: To achieve a natural appearance, a low-frequency Gaussian noise field is applied to the surface, and radial sharp-angled spikes are added.

- *Morphological Refinement*: The final stage employs morphological filtering to ensure fragment integrity.

- *Binary Closing*: Fills small undesirable internal voids.

- **Binary Opening:** Removes small "noise" and isolated pixels around the shape. Largest Connected Component: Identifies the largest contiguous object and removes all isolated points resulting from noise.

2) **Spatial Adaptation, Positioning, and FB Insertion:** the algorithm prepares the "scene" for the 3D model insertion:

- **Resampling:** Since the generator's voxel grid (e.g., 0.5 mm isotropic) may differ from the CT scan's resolution (e.g., 1.0 x 1.0 x 0.8 mm), the fragment's 3D model is adjusted to the specific CT resolution using interpolation.

- **Intelligent Placement:** A center point for the FB model is selected. Instead of a purely random selection, the method utilizes an Euclidean Distance Transform (EDT) on the randomly selected mask of one of the four cardiac chambers masks

$$M_{heart} = \{M_i^{(lv)}, M_i^{(la)}, M_i^{(rv)}, M_i^{(ra)}\}_{i=1}^{N_{clean}}.$$

This ensures the fragment is placed deep enough within the chamber to fit entirely within its boundaries.

3) **Physically Grounded HU Filling (Heterogeneous Appearance):** A metallic FB on a CT scan does not consist of voxels with a single uniform HU value. The algorithm simulates the following physical properties:

- **High Density:** HU values are set within the range of +1800 to +12000 (typical for steel, aluminum, and other metals).

- **Heterogeneity:** Random Gaussian noise and a "hotspot" at the fragment's center are added to simulate non-uniform photon absorption relative to the object's thickness.

4) **Metal Artifact Generation:** This is the most critical step for realism. Since metal causes X-ray scattering and photon starvation, artifacts are added to each 2D slice containing the FB. While not perfect physical replicas of specific scanner physics, they are heuristically and statistically consistent with common CT artifacts through the following steps:

- **Radial Streaks:** 5 to 18 radial rays are generated from the fragment's center.

- **Bright/Dark Rays:** Some rays are rendered bright (scattering, reconstruction errors), while others are dark (photon starvation).

- **Angular Jitter:** Random angular displacement of the rays is applied to ensure a natural and chaotic appearance.

5) **Physical Blending and Storage:**

- **Local Blur:** The boundaries between metal and tissue are softened using a Gaussian filter. This simulates the partial volume effect, where object boundaries do not align perfectly with voxel edges.

- **Saturation Simulation:** Each voxel's HU value is clipped at the +3071 HU threshold.

- **Mask Preservation:** Simultaneously with the modified CT, an ideal binary fragment mask is generated for training machine learning models.

The schematic diagram of the MorphGenFB-CT method is shown in Fig. 3.

Below are the slices of artificially synthesized CT images of cardiothoracic injuries with a metallic foreign body (FB) localized in the left ventricle, generated using the RealInsFB-CT (Fig. 4) and MorphGenFB-CT methods (Fig. 5 – insertion of a synthetic FB without artifacts; Fig. 6 – insertion of a synthetic FB with artifacts). These can be compared with a real-world cardiothoracic injury CT scan (Fig. 7).

All real-world CT scans were performed using the same equipment. All CT datasets (real-world with FBs, "clean" real-world, and synthetic) are anatomically constrained between the upper part of the L1 vertebra inferiorly and the jugular notch superiorly, covering the same body regions and organs. Figure 8 illustrates the 3D FB model that was inserted into the CT scan in Fig. 5 during synthesis via the MorphGenFB-CT method.

Additionally, averaged HU (Hounsfield Unit) density distribution histograms were constructed for:

1) A set of 8 real-world CT scans containing 19 FBs.

2) A set of 19 CT scans (one FB per scan) synthesized using the RealInsFB-CT and MorphGenFB-CT methods based on 4 "clean" CT scans (Figs. 10–12).

Furthermore, similar averaged histograms were generated for the Regions of Interest (ROIs) across all three CT sets, specifically encompassing only the foreign body, visible artifacts, and the immediate surrounding tissues (Figs. 13–15).

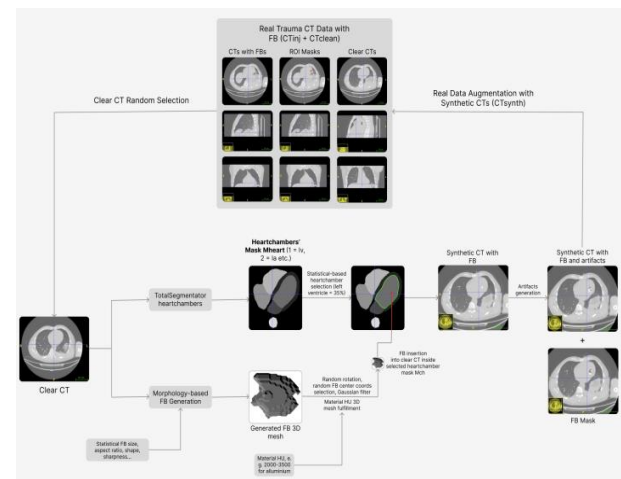


Fig. 3. MorphGenFB-CT method

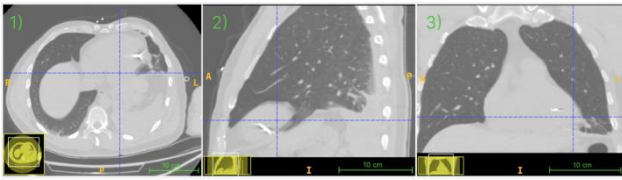


Fig. 4. Synthetic CT scan generated using the ReallnsFB-CT method: (1) is the axial; (2) is a sagittal; (3) is the coronal

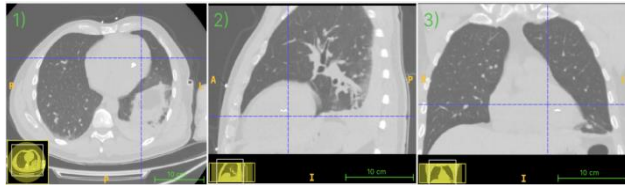


Fig. 5. Synthetic CT scan generated using the MorphGenFB-CT method with FB, without artifacts: (1) is the axial; (2) is a sagittal; (3) is the coronal

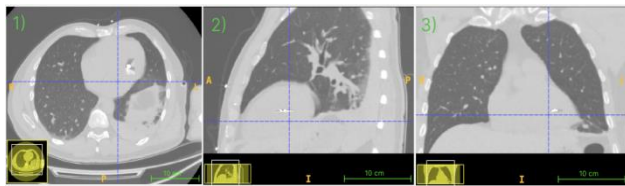


Fig. 6. Synthetic CT scan generated using the MorphGenFB-CT method with FB and artifacts: (1) is the axial; (2) is a sagittal; (3) is the coronal

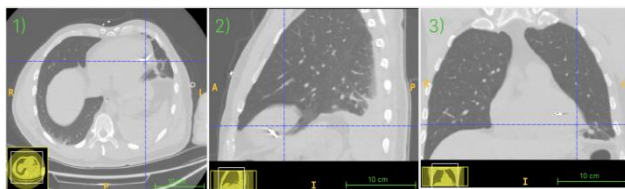


Fig. 7. Real CT scan: (1) is the axial; (2) is a sagittal; (3) is the coronal

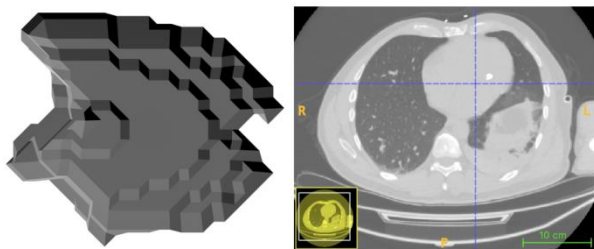


Fig. 8. 3D model of the foreign body and the result of its insertion into a "clean" CT scan

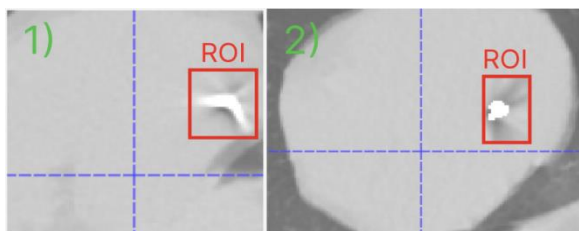


Fig. 9. ROIs for: (1) is the ReallnsFB-CT method; (2) is the MorphGenFB-CT method

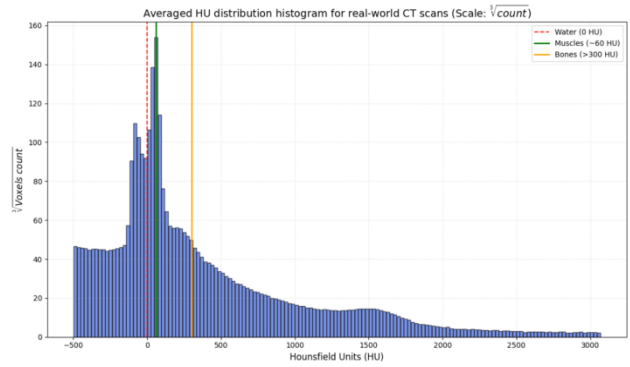


Fig. 10. Averaged HU distribution histogram for real-world CT scans

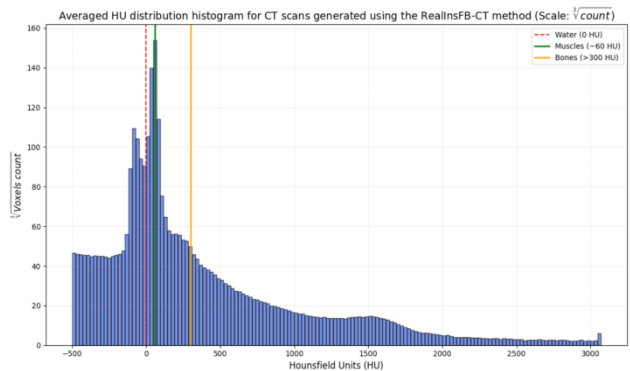


Fig. 11. Averaged HU distribution histogram for CT scans generated using the ReallnsFB-CT method

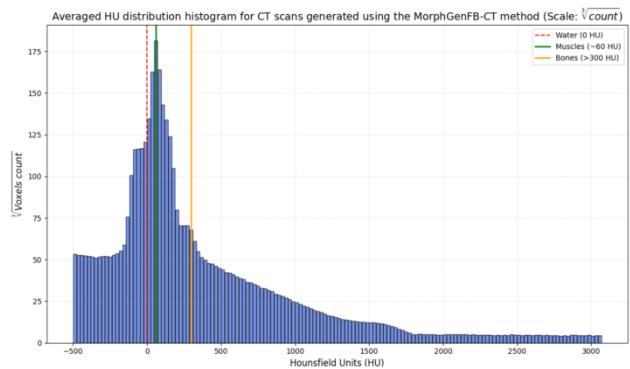


Fig. 12. Averaged HU distribution histogram for CT scans generated using the MorphGenFB-CT method

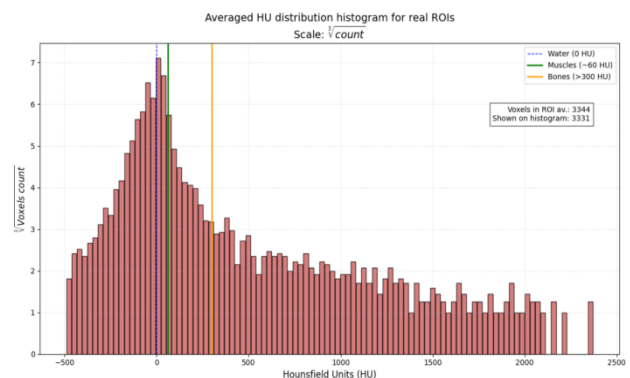


Fig. 13. Averaged HU distribution histogram for real ROIs

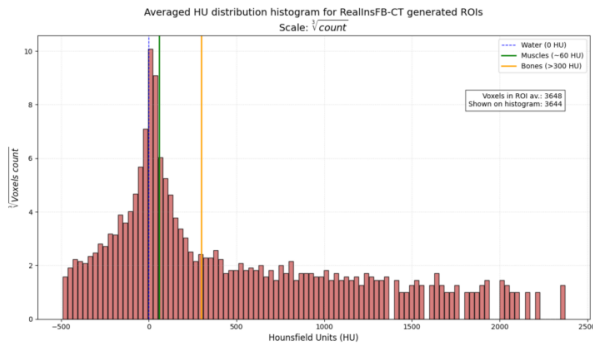


Fig. 14. Averaged HU distribution histogram for RealInsFB-CT generated ROIs

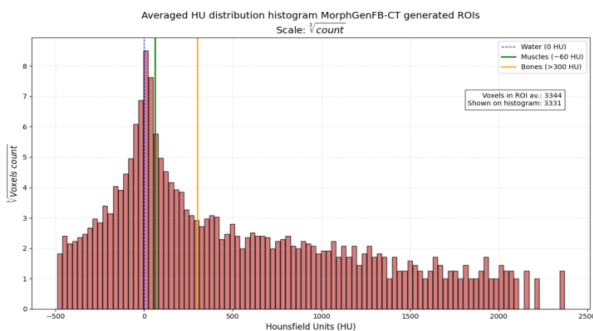


Fig. 15. Averaged HU distribution histogram for MorphGenFB-CT generated ROIs

The histograms demonstrate a nearly identical averaged HU distribution for the real-world CT datasets and the CT sets synthesized using the RealInsFB-CT and MorphGenFB-CT methods, indicating the statistical similarity between the real and synthetic data. The distribution of HU values corresponding to soft tissues and fluids differs slightly between the real-world CT set and the set synthesized via the RealInsFB-CT method. This discrepancy is attributed to the inherent differences between the "clean" real-world CT scans used for synthesis and the original injury scans, as well as the fact that the RealInsFB-CT method involves extracting not only the foreign body mask but also the surrounding tissues and artifacts for insertion into the donor scan.

A comparison of the CT slices synthesized using the RealInsFB-CT and MorphGenFB-CT methods with real-world CT scans confirms that they are visually and structurally similar, exhibiting nearly identical streaking and starburst artifacts.

V.CONCLUSIONS

Based on the analysis of scientific publications and the study of combat cardiothoracic trauma statistics, the importance of developing tools for the segmentation of foreign bodies (FBs) (bullets, fragments, etc.) in the heart via CT was substantiated. The necessity of employing machine

learning models within such tools was established, as conventional analytical methods (HU thresholding, adaptive filtering) fail to effectively segment foreign bodies in the presence of artifacts and saturation effects. Furthermore, the need for synthetic CT image generation to augment the scarce real-world datasets required for training 3D U-Net or ViT-based architectures to improve segmentation accuracy was addressed.

The morphology of foreign bodies localized in the cardiac region during combat cardiothoracic traumas was studied. A small dataset was compiled, consisting of 8 CT scans of cardiothoracic injuries with FBs localized in the cardiac area and 4 "clean" CT scans of patients with blast-induced injuries who lacked foreign bodies in the heart region.

Two methods for synthesizing artificial CT scans of cardiothoracic injuries (RealInsFB-CT and MorphGenFB-CT) were developed, and the visual, structural, and statistical similarity of synthesized and real-world CT scans was demonstrated.

The advantage of the RealInsFB-CT method lies in its use of foreign body images extracted directly from real CT scans.

The advantage of the MorphGenFB-CT method is its applicability even in the absence of real FB images, relying solely on statistical and morphological data, alongside the flexibility to select FB materials during the 3D model voxel-filling stage.

A limitation of the RealInsFB-CT method is the necessity of extracting not only the foreign body itself but also the surrounding tissues and artifacts. This restricts the number of potential implantation sites while maintaining anatomical consistency and renders the synthesis of cardiac FB scans using fragments extracted from other organs less effective due to discrepancies in tissue structure and radiologic density. A shared limitation of both methods is the lack of modeling for tissue deformation and structural changes caused by the injury (e.g., wound channels, hematomas, or free fluid from hemorrhages), although such changes are often obscured by artifacts.

Future research may involve the development of a hybrid method that extracts only the fragment from a real CT scan (RealInsFB-CT approach), inserts it into a "clean" CT, and then simulates artifacts around it (MorphGenFB-CT approach). However, such a method would require a large number of precisely labeled fragments, which remains a significant challenge. Additionally, a comparative study of neural network models (specifically using the nnU-Net framework) can be conducted by

training on various dataset types: exclusively on limited real-world CT images versus mixed datasets (real + synthetic CT) utilizing the proposed synthetic augmentation methods.

REFERENCES

- [1] B. Biocina, et al., "Penetrating cardiothoracic war wounds", 1996. [https://doi.org/10.1016/S1010-7940\(96\)01124-4](https://doi.org/10.1016/S1010-7940(96)01124-4)
- [2] V. H. Hetman, et al., "Foreign Bodies of the Thorax after Combat Trauma", 2017.
- [3] R.Ya. Abdullaev, et al., "Radiological diagnosis of damage to the heart and large chest vessels in combat trauma", 2025. <https://doi.org/10.34921/amj.2025.1.011>
- [4] A. Uluhan, et al., "Single center experience of war-related thoracic injuries in Syria", 2017. <https://doi.org/10.26663/cts.2023.0015>
- [5] Eshan L. Senanayakea, Henrietta Poonc, Tim R. Grahama and Mark J. Midwinter, "UK specialist cardiothoracic management of thoracic injuries in military casualties sustained in the wars in Iraq and Afghanistan", 2014. <https://doi.org/10.1093/ejcts/ezu076>
- [6] Matthew A Borgman, Philip C Spinella, Jeremy G Perkins, Kurt W Grathwohl, Thomas Repine, Alec C Beekley, James Sebesta, Donald Jenkins, Charles E. Wade, John B. Holcomb, "The ratio of blood products transfused affects mortality in patients receiving massive transfusions at a combat support hospital," 2007, <https://doi.org/10.1097/ta.0b013e3181271ba3>.
- [7] J. A. Asensio, J. Murray, D. Demetriades, J. Berne, E. Cornwell, G. Velmahos, H. Gomez, and T. V. Berne, "Penetrating cardiac injuries: a prospective study of variables predicting outcomes," 1998 [https://doi.org/10.1016/s1072-7515\(97\)00144-0](https://doi.org/10.1016/s1072-7515(97)00144-0).
- [8] Federico M. Bella, Alessandra Bonfichi, Ciro Esposito, Christian Zanza, Abdelouhab Bellou, Domenico Sfondrini, Antonio Voza, Andrea Piccioni, Antonio Di Sabatino, and Gabriele Savioli, "Extended Focused Assessment with Sonography for Trauma in the Emergency Department: A Comprehensive Review," 2025. <https://doi.org/10.3390/jcm14103457>
- [9] Ya. L. Zarutskyi, & O. S. Shudra, "Military Field Surgery: A Textbook," Kyiv: Fenix, 2020.
- [10] I. P. Khomenko, et al., "Specifics of providing specialized medical care for combat heart wounds." *Surgery of Ukraine*, pp. 12–18 no. 2, 2023.
- [11] L. B. Balsam, et al., "The American Association for Thoracic Surgery (AATS) 2021 Expert Consensus Document: Management of penetrating thoracic trauma. The Journal of Thoracic and Cardiovascular Surgery, 162(5), 1431–1444", 2021.
- [12] D. F. Szpisjak, et al., "Emergency War Surgery (5th US Revision). US Army Medical Center of Excellence", 2022.
- [13] Carlin Lee, Mallory Jebbia, Raveendra Morchi, Areg Grigorian, Jeffry Nahmias, "Cardiac Trauma: A Review of Penetrating and Blunt Cardiac Injuries," 2024. <https://doi.org/10.1177/00031348241307400>
- [14] H. Ihnatenko, et al., "Surgical strategy for foreign body removal from the heart in combat casualties," *Journal of Military Medicine*, 2024.
- [15] John Breeze, C. J. Steel, A. Breize, and K. M. Sarber, "Characterisation of retained energised fragments from explosive devices in military personnel," 2022. <https://doi.org/10.1136/bmjmilitary-2021-001825>
- [16] Abstracts of the Young Scientists' Conference of the Ukrainian Military Medical Academy (UMMA): "Current Aspects of Military Healthcare – Scientific Achievements of Youth", 2026.
- [17] Fabian Isensee, Jens Petersen et al., "nnU-Net: Self-adapting Framework for U-Net-Based Medical Image Segmentation", 2018. <https://doi.org/10.48550/arXiv.1809.10486>
- [18] Eric J. Snider, Sofia I. Hernandez-Torres and Emily N. Boice, "An image classification deep-learning algorithm for shrapnel detection from ultrasound images", 2022. <https://doi.org/10.1038/s41598-022-12367-2>
- [19] Cheng-Yi Li, Haoyue Guan, and Jiashu Cheng, "Dataset and Benchmark for Enhancing Critical Retained Foreign Object Detection," 2025. <https://doi.org/10.48550/arXiv.2507.06937>
- [20] Jacob Wasserthal, Hanns-Christian Breit, Manfred T. Meyer, "TotalSegmentator: robust segmentation of 104 anatomical structures in CT images," 2022. <https://doi.org/10.48550/arXiv.2208.05868>

Received: February 06, 2026

Accepted: March 13, 2026

Published: April 18, 2026

Kosiuk Oleksii. ORCID 0009-0001-6647-9558. Postgraduate Student.

Department of Artificial Intelligence, Educational and Research Institute for Applied System Analysis, National Technical University of Ukraine "Ihor Sikorsky Kyiv Polytechnic Institute," Kyiv, Ukraine

Research interests: synthetic data generation, artificial neural networks.

Publications: 1.

E-mail: kosiuk.o.m.-ki51f@edu.kpi.ua

Chumachenko Olena. ORCID 0000-0003-3006-7460. Doctor of Engineering Science. Professor.

Department of Artificial Intelligence, Educational and Research Institute for Applied System Analysis, National Technical University of Ukraine "Ihor Sikorsky Kyiv Polytechnic Institute," Kyiv, Ukraine.

Education: Georgian Polytechnic Institute, Tbilisi, Georgia, (1980).

Research area: system analysis, artificial neural networks.

Publications: more than 80 papers.

E-mail: chumachenko@tk.kpi.ua

О. М. Косюк, О. І. Чумаченко. Генерація синтетичних КТ-зображень поранених із локалізацією сторонніх тіл у серці

Статтю присвячено генерації синтетичних КТ-зображень кардіоторакальних поранень зі сторонніми тілами (СТ), локалізованими в області серця, що може бути корисним зокрема для покращення точності сегментації СТ моделями машинного навчання шляхом доповнення навчальних датасетів синтетичними зображеннями. Зібрано невеликий набір реальних даних, що складається з 8-ми КТ бойових кардіоторакальних поранень з локалізацією сторонніх тіл (від 1 до 3) в області серця, та ще 4-х чистих КТ мінно-вибухових кардіоторакальних поранень, на яких сторонні тіла в області серця відсутні. За допомогою аналізу зібраного датасету та результатів схожих досліджень вивчено морфологію сторонніх тіл і статистику їх локалізації в серці при бойових кардіоторакальних травмах. Розроблено 2 методи синтезу штучних КТ-зображень кардіоторакальних поранень з локалізацією СТ у серці на базі чистих КТ: RealInsFB-СТ, заснований на вставці екстрагованих з реальних КТ поранень фрагментів (ROI), які містять СТ, артефакти та навколишні пошкоджені тканини, у чисті КТ і MorphGenFB-СТ, заснований на морфологічно та статистично обґрунтованій штучній генерації 3D-моделі СТ, заповнення моделі значеннями HU, які відповідають обраному матеріалу СТ, вставці моделі в одну з камер серця на чистому КТ та штучній генерації артефактів. За допомогою обох методів синтезовано КТ-зображення, зібрані у навчальні набори даних (по 19 КТ + 19 масок СТ у кожному). Доведено візуальну, структурну та статистичну схожість реальних та штучно синтезованих КТ.

Ключові слова: синтетичні дані, доповнення даних, кардіоторакальна травма, сегментація, сторонні тіла, комп'ютерна томографія.

Косюк Олексій Михайлович. ORCID 0009-0001-6647-9558. Аспірант.

Кафедра штучного інтелекту, Навчально-науковий інститут прикладного системного аналізу, Національний технічний університет України «Київський політехнічний інститут ім. Ігоря Сікорського», Київ, Україна.

Напрямок наукової діяльності: генерація синтетичних даних, штучні нейронні мережі.

Кількість публікацій: 1.

E-mail: kosiuk.o.m.-ki51f@edu.kpi.ua

Чумаченко Олена Іллівна. ORCID 0000-0003-3006-7460. Доктор технічних наук. Професор.

Кафедра штучного інтелекту, Навчально-науковий інститут прикладного системного аналізу, Національний технічний університет України «Київський політехнічний інститут ім. Ігоря Сікорського», Київ, Україна.

Освіта: Грузинський політехнічний інститут, Тбілісі, Грузія, (1980).

Напрямок наукової діяльності: системний аналіз, штучні нейронні мережі.

Кількість публікацій: більше 80 наукових робіт.

E-mail: chumachenko@tk.kpi.ua